Title	Summary of Component Design Report		
Document No.	DE-EE0006610 M6.1c Summary of Component Design Report		
Version	1.0		
Prime Contract	DE-EE0006610		
Authored	K. O'Hearn		
Reviewed	P. Lenee-Bluhm, M. Ondusko		
Version Approved			
Data Classification	☐ Limited Rights Data	☒ Protected Data	☐ Public Data

Version	Date	Summary
1.0	11/26/19	Release with Final Reporting

TABLE OF CONTENTS

1 INTRODUCTION 1
2 NEXT-GENERATION PROTOTYPE HULL DESIGN 1
3 GEOMETRIC AREAS OF INTEREST FOR FURTHER DEVELOPMENT 11
4 MIXED MATERIAL PONTOON CONCEPT DESIGN 14
5 CONCLUSION 20
6 REFERENCES 21

TABLE OF FIGURES

Figure 1 – StingRAY H1 and H2 architectures. 2
Figure 2 – Depiction of the finite element model and boundary conditions. 4
Figure 3 – Von Mises stress of aft, inboard side of forward pontoon joint. 7
Figure 4 – Von Mises stress of forward pontoon joint, with closeup (shell removed for clarity). 8
Figure 5 – Lifting and rigging. 10
Figure 6 - Foundation pedestals. 11
Figure 7 – Criteria for the selection of geometric areas of interest for further optimization. 12
Figure 8 – Tsai Wu Failure Criterion (DNVGL-ST-C501). 14
Figure 9 – Pontoon finite element model (FEM). 15
Figure 10 – Hydrostatic pressure load case applied forces vary with depth. 16
Figure 11 – Slamming load case applied forces are constant. 16
Figure 12 – Resultant bondline force vectors at the near-end boundary conditions, load case 6. 19
Figure 13 – Double lap shear joint detail. 19

TABLE OF TABLES

Table 1 – Assumed properties for structural elements. 3
Table 2 – H2 structural component design loads. 5
Table 3 – Calculated fatigue life. 7
Table 4 – Calculated fatigue life with weld profiling. 9
Table 5 – Concept pontoon design load cases. 15
Table 6 – Maximum TWFC summary. 18
Table 7 – Bondline stresses. 18

1 INTRODUCTION

In a successful collaborative Department of Energy project, Columbia Power Technologies, Inc. (C·Power), along with the National Renewable Energy Laboratory (NREL), Glosten Navel Engineering, and multiple composite design and fabrication companies completed the Project resulting in significant data to allow for hull structure mass and cost reduction in the StingRAY Wave Energy Converter (WEC) hull. The steel and fiber-reinforced plastic (FRP) mixed materials design was developed by Glosten, C·Power, and Ershigs. Fabrication of the composite materials for testing was provided by Ershigs and Corrosion Companies Inc. Huntsman and ITW Performance Polymers provided adhesive recommendations and products to test. Research validation structural testing was developed and conducted by NREL at the National Wind Technology Center (NWTC) in Boulder, CO.

Outside of the DE-EE0006610 (6610) Project, the H2 prototype hull concept was developed in-house using the hydrodynamic modeling software ANSYS AQWA and sea state data provided by University of Hawaii for deployment at the Navy's Wave Energy Test Site (WETS) located in Kaneohe Bay, Hawaii and connected to the Hawaiian power grid through Marine Corps Base Hawaii (MCBH).

Within 6610 the StingRAY next-generation H2 prototype hull concept was further developed into a complete structural design by Glosten, a marine engineering firm located in Seattle Washington. C·Power provided loading time history (developed in AQWA) and Engineering Design Requirement (EDR) documents (which specified the requirements for the operation and deployment of the H2). Glosten provided a structural hull design of the H2 WEC with a minimum life span of five years and capable of surviving a 50-year storm at WETS.

After completion of the H2 hull design, Glosten and C·Power engineers collaborated in identifying multiple Geometric Areas of Interest (GAIs) for further research and development which could possibly reduce the overall mass of the hull structure while reducing fabrication costs. After identifying several areas of possible further development that matched the selection criteria, they were down-selected to the implementation of hybrid material pontoon construction. The modified pontoons would have the greatest potential for cost and mass reductions while not limiting the ability to make rapid design and structural changes to the WEC generator housing, a principal design requirement for prototype development. Furthermore, there are several hull components with significant structural similarities to the pontoon, and it is reasonable to assume that a similar hybrid construction could readily be adapted for these components as well.

With fabrication consideration at the forefront of the design development, the concept structural changes were evaluated for integration into the current hull structure design. The joining of composite sections to the steel structure on a marine device showed the highest likelihood of failure during fabrication and deployment, and least applicable reference information and thus was selected for full-scale testing to expose unknown variables and provide information to specify achievable fabrication tolerances and procedures.

The purpose of this document is to summarize the H2 hull and concept hybrid pontoon design activities performed in Project tasks 3.1 to 3.4 (identified in 6610 Project Statement of Project Objectives, mod 4).

2 NEXT-GENERATION PROTOTYPE HULL DESIGN

The StingRAY WEC has undergone a generational advancement. Developed under DE-EE0005390, the StingRAY H1 was examined for cost reduction opportunities in conjunction with DE-EE0007347. Using ANSYS AQWA, numerous design concepts were evaluated. It was determined the aft float and generator pair were harvesting about a third of the energy captured by the front float and generator. Further, H1's

damper plate, which was to be solid steel, came under scrutiny for its cost and operational challenges it presented to float it during deployment and recovery. The result was a two-body WEC (H2) comprised primarily of cylindrical shell structures.

The H2 concept centers about an architecture that allows for more efficient use of structural and power generation components, along with simplified component geometries aimed at reducing manufacturing costs; these changes result in lower cost and weight. The new H2 architecture also exhibits a significant improvement in power performance. The H2 WEC can transition between floating tow and power production configurations via a seawater ballast change, without the need for at-sea installation of external buoyancy components which were required by H1, reducing operations complexity and cost. The original H1 and improved H2 architectures are shown in Figure 1.

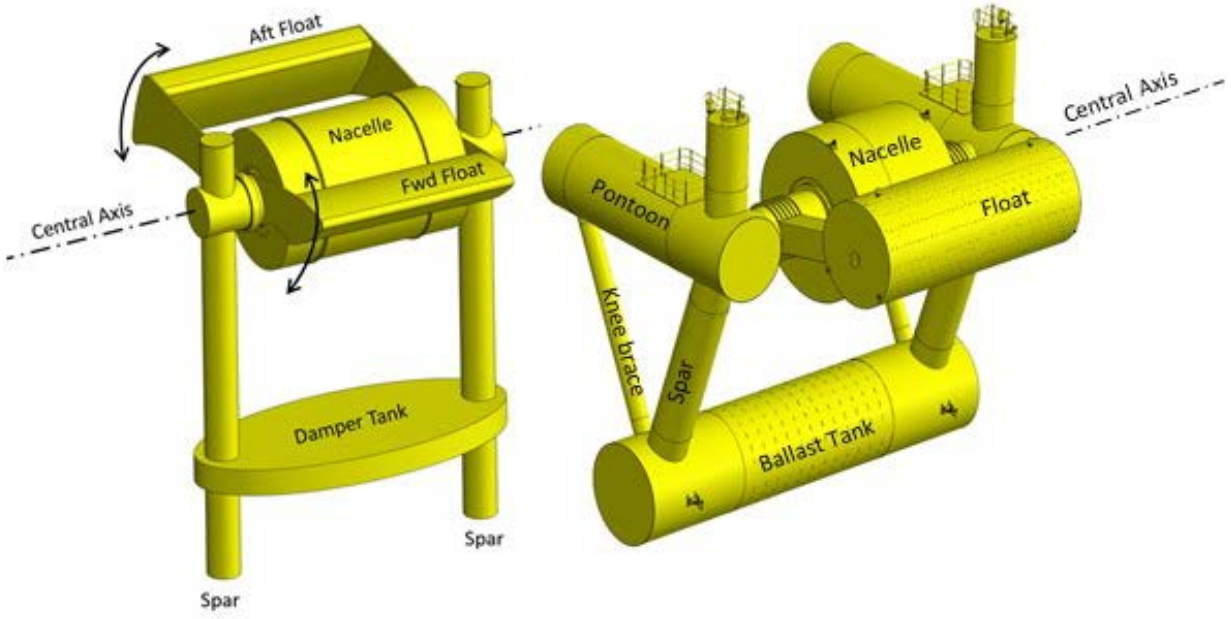

Figure 1 – StingRAY H1 and H2 architectures.

C·Power numerical modeling provided the mass and geometric requirements of the hull for optimal performance, specific to the WETS location; the concept design was an idealized geometry and was progressed to a detailed design under the Project.

Design load cases were specified for the WETS test site, guided by *IEC 62600-2 Design requirements for marine energy systems* [1]. Detailed description of the DLCs and justification of their selection is covered in *M2.1-Design Load Cases for Structural Optimization* [2].

Loads were assessed computationally using fully coupled time-domain numerical simulations, accounting for all load contributions simultaneously (ANSYS AQWA-NAUT v16). All relevant loads were considered in the calculations, including hydrodynamic loading, inertial loading, and functional loading from PTO and mooring. The hydrodynamic loads include hydrostatic, Froude-Krylov, viscous drag, added mass, and drift forces. Details of model set up, and description of loads and other outputs, are given in *SR-Design Loads* [3].

C·Power provided the time series loads and accelerations, along with Engineering Design Requirements, to Glosten, a naval architecture and engineering firm in Seattle, WA so that a detailed design closely replicating the concept could be developed.

The H2 hull structure was designed entirely from steel to accommodate fabrication as well as modification and design flexibility to the generator housing. The hull structure design was constrained by a requirement for the device to be able to be towed without external/auxiliary buoyancy for deployment and recovery, as well as requiring a minimum 5-year design life and surviving a 50-year storm at the deployed location.

A total of 10 x 3-hour simulations were run for power production (damped) mode in extreme seas, and another 10 x 3-hour simulations for freewheeling (undamped) in extreme seas. Each simulation had a unique set of random phase angles for the spectral components. The seas were modeled with directional spreading, but with the mean direction head-on to the WEC (as the single point mooring allows the WEC to align itself with the waves). Two additional 3-hour simulations were run for a bimodal extreme seas, one in power production mode and one freewheeling. The bidirectional sea state had the same overall significant wave height and energy period but split the waves into wind and swell components that were separated directionally by 90°.

After reviewing the simulation data, Glosten down-selected from the twenty head-on cases to the eight worst-case simulations, considering both maximum body motions and maximum joint loads. A total of ten simulations (four head-on power production, four head-on freewheeling, and both bidirectional cases) were used to derive design loads.

The pre-screened simulations were evaluated with a brute force finite element analysis (FEA) at each time step. This finite element model was created in Nx Nastran using massless beam elements with cylindrical tube sections. The analysis assumes an unstiffened cross-section with rule minimum thicknesses for the tube walls in order to approximate the relative stiffness between members. The assumed properties of each structural element were defined as per Table 1 below. Material properties were defined as AH36 steel per the American Bureau of Shipping (ABS) standards with Elastic Modulus at 2.06E+11 and a Poisson's Ratio of 0.3.

Table 1 – Assumed properties for structural elements.

Structure	Radius	Thickness
Nacelle	3.8	0.007
Nacelle Tube	1.125	0.007
Pontoon P	1.913	0.007
Pontoon S	1.913	0.007
Ballast Tank	2.35	0.007
Upper Spar P	1	0.007
Upper Spar S	1	0.007
Knee Brace P	0.483	0.007
Knee Brace S	0.483	0.007
Lower Spar P	1	0.007
Lower Spar S	1	0.007

The mass of each structural element was modeled as a point mass located at the center of gravity. Rigid mass nodes were attached to the beam elements. The port and starboard lower spars and knee braces in the AQWA simulations were modeled as single elements. The mass and inertia for these elements were split into port and starboard elements for the FEA to achieve the same total mass and inertia of the central body.

An illustration of the finite element model and boundary conditions can be seen in Figure 2. Each load case is dynamically balanced with the calculated acceleration and velocities from the simulation time step. Therefore, the global restraints shown at the end of the pontoons are only necessary to constrain the

slight imbalance between loads and inertia. Constrained reaction forces and moments are small, on the order of 20 kN and 10 kNm respectively.

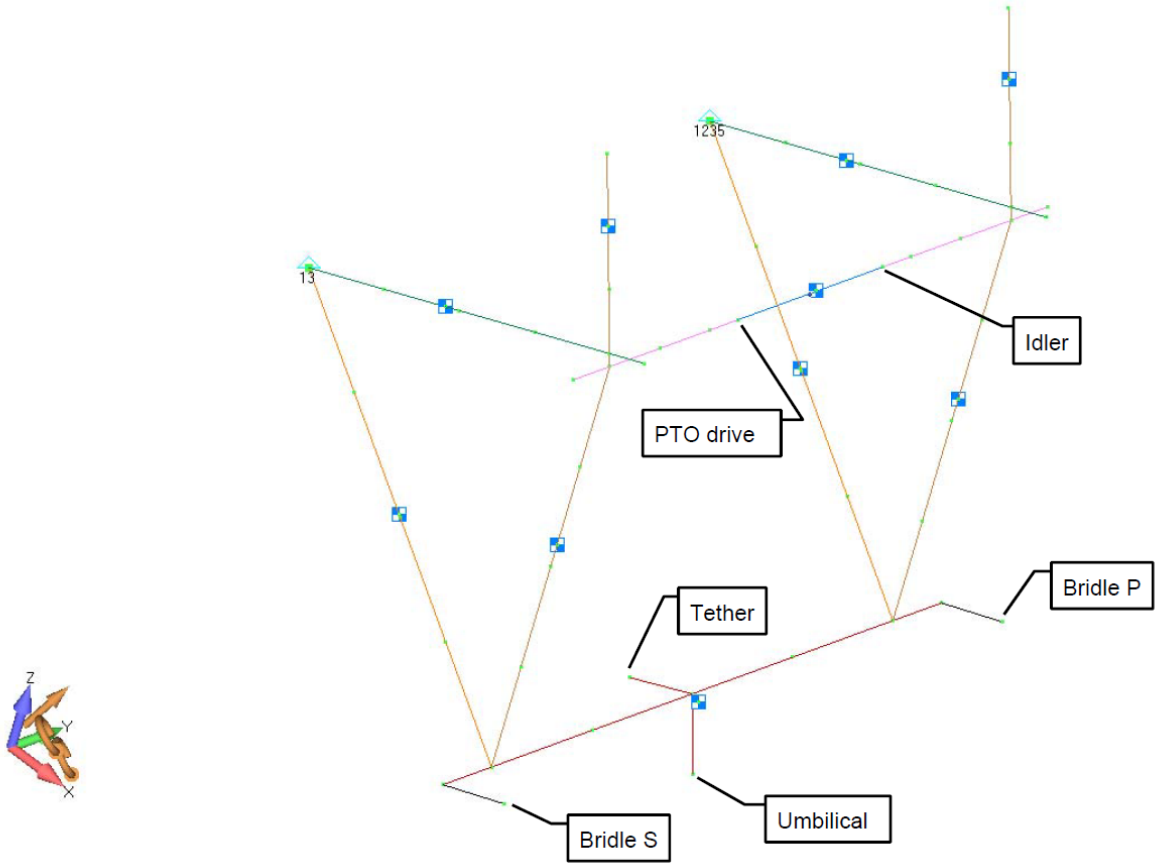

Figure 2 – Depiction of the finite element model and boundary conditions.

Functional loads for StingRAY hull design were developed by applying loads from the PTO and float arm joint at the float arm interface rather than the center of gravity of the nacelle. The PTO drive node is assumed to carry all moment and thrust. Radial loads from the float arm were divided between the drive side and idler side nodes. The bridle, tether, and umbilical forces were applied at the mooring attachment points identified. The nodes representing the bridle points were connected to the beam model using rigid elements. The tether and umbilical were attached using stiff beams with a cross-section equal to the ballast tank.

The finite element model was loaded and analyzed for the extreme sea state in a total of ten 3-hr simulations, including four 3-hr simulations for the damped condition, four 3-hr simulations for the undamped condition, one 3-hr bi-directional wind/wave simulations damped, and one 3-hr bidirectional wind/wave case undamped. Every other time step in the simulation was evaluated in order to keep file size and analysis time within manageable limits. The results were post-processed to identify the maximum and minimum bending moment, axial force, shear, and torsion in each of the structural elements of the AQWA model. The structural design load maximums with the concurrent loads at that time step are provided in Table 2.

Table 2 – H2 structural component design loads.

Design Force and Moments - Extreme Seas							
	Notes:						
	1) *Bending moments and shear are provided as vector sum of values for local y and z element axes.						
	(Local element x-axis is in axial direction of each cylinder.)						
	2) One concurrent load case provided that maximizes each process.						
	3) Time in simulation = isub*0.1111 seconds.						
	4) Maximum values for any seed presented without averaging or partial safety factors.						
	5) FEA model assumes the drive arm side of the nacelle tube carries the entire moment.						
Process -->	**Bending Moment***	**Shear***	**Axial Force**	**Axial Force**	**Total Torque**		
Body	**[kNm]**	**[kN]**	**Max [kN]**	**Min [kN]**	**[kNm]**	**Source**	**isub**
Nacelle	**8557**	1025	—	-59	-23	5D_Nacelle	19524
Nacelle	8022	**1082**	—	-220	427	BiDirU_Nacelle	69688
Nacelle	5403	516	**611**	—	-166	BiDirU_Nacelle	89040
Nacelle	1947	383	—	**-646**	-485	BiDirD_Nacelle	90572
Nacelle	2651	568	—	-423	**1932**	BiDirD_Nacelle	50502
Nacelle Tube	**6073**	683	—	-303	-1737	10D_NacelleTube	7350
Nacelle Tube	605	**1144**	—	-84	192	BiDirD_NacelleTube	88970
Nacelle Tube	5012	516	**611**	—	-128	BiDirU_NacelleTube	89040
Nacelle Tube	3720	357	—	**-767**	-1028	BiDirU_NacelleTube	90572
Nacelle Tube	2710	663	—	-453	**1932**	BiDirD_NacelleTube	50502
Pontoon	**7755**	876	—	-161	35	10D_Pontoon	51312
Pontoon	4761	**894**	—	-497	48	6U_Pontoon	94862
Pontoon	3601	619	**468**	—	-152	5U_Pontoon	44820
Pontoon	518	426	—	**-866**	64	6U_Pontoon	45216
Pontoon	705	372	—	-155	**299**	BiDirD_Pontoon	62278
BallastTk	**18977**	2342	—	-67	954	BiDirD_BallastTk	88972
BallastTk	1812	**2373**	128	—	-1220	BiDirD_BallastTk	69692
BallastTk	3281	2080	**347**	—	-347	BiDirU_BallastTk	33222
BallastTk	3224	704	—	**-461**	-2386	10D_BallastTk	7350
BallastTk	634	520	89	—	**2307**	BiDirD_BallastTk	89030
UpperSpar	**511**	121	108	—	0	7U_UpperSpar	53772
UpperSpar	108	**148**	-59	—	-1	BiDirD_UpperSpar	92622
UpperSpar	67	58	**116**	—	1	7U_UpperSpar	53550
UpperSpar	181	35	—	**-100**	-1	BiDirD_UpperSpar	43644
UpperSpar	46	8	12	—	3	BiDirD_UpperSpar	71916
LowerSpar	**3203**	362	1108	—	-92	BiDirU_LowerSpar	89068
LowerSpar	2855	**418**	827	—	1487	10D_LowerSpar	7350
LowerSpar	1131	120	**1856**	—	227	BiDirD_LowerSpar	88970
LowerSpar	660	126	—	**-839**	-71	6U_LowerSpar	88530
LowerSpar	665	401	631	—	**1501**	10D_LowerSpar	7350
KneeBrace	**1019**	112	—	-227	174	10D_KneeBrace	7350
KneeBrace	193	**122**	—	-281	178	10D_KneeBrace	7350
KneeBrace	7	29	**1096**	—	34	3D_KneeBrace	30132
KneeBrace	121	38	—	**-382**	-71	10D_KneeBrace	33664
KneeBrace	287	53	223	—	**253**	BiDirU_KneeBrace	22606

The original intent of the 10 simulations was to provide data for statistical evaluation of the loads. This approach was abandoned in favor of providing concurrent balanced load sets for structural design to maximize each process of interest. The results indicated that the bidirectional cases governed many load processes, so a statistical approach was not possible in those cases and the adopted approach lent consistency. The maximum local design pressures from depth and slamming developed by C·Power were not included loadings in this iteration of FEA, but they were included as loads in the follow-on design calculations.

The shell plate thickness of members subjected to slamming (i.e., those members at or above the free surface) were evaluated. Slamming loads for the upper spar, lower spar, and knee brace were taken as the greater of side shell sea loading. Exposed deck loading or lowest tier forward external superstructure bulkheads pressure was applied over a 60° arc for conservatism. This approach accounted for the global stresses by a proportional reduction in design bending stress. A correction factor for curved plates was applied to the required thickness for unstiffened shells. An FEA was developed to check the nacelle,

pontoon and float ring frames against the slamming loads. The beam ends were defined as a 60° arc as this is considered self-supporting and fixed. Pressure was applied over the arc and a PSF of 1.5 was applied to the pressure values and a material PSF of 1.15 is assumed. Solidworks simulations were used to evaluate and validate the slamming pressure on the ring frames and unstiffened shell sections.

After the completion of the superstructure analysis, a local analysis of the primary structural joints rounded out the StingRAY H2 hull design. A Solidworks simulation FEA was performed on the following joints as there were no available stress concentration factors for the specific arrangements:

- pontoon, nacelle tube, main spar, and upper spar joint
- pontoon and knee brace joint
- ballast tank, main spar, and knee brace joint

The finite element model consisted of the primary members modeled to half span where it was fixed. The intersecting members were modeled to a point 1 meter from the intersection to the primary members. The loads from the case that resulted in the highest global stress were applied to each intersecting member respectively. Artificial axial, bending, and torsional loads were applied at the free end bulkhead. These were assumed as a 1" thick rigid plate to ensure uniform load transfer of the primary member. Shear loads were evaluated at the bulkhead in way of the joint, such that the reaction at the fixed end was equivalent to the worst-case free body loads in order to develop the corresponding far-field stresses.

The fatigue assessment for the prototype WEC structure was carried out by Glosten in accordance with DNV-GL and C-Power design requirements guidance. Table 3 contains hot spot stresses calculated from detailed finite element analysis results according to *DNV-RP-C203 Fatigue Design of Offshore Steel Structures* [4] for the three tubular joint models. Table 3 lists the calculated fatigue life for the tubular joint details calculated as a Miner's sum, assuming a Weibull shape factor of 1.0 and an S-N curve for tubular joints (*DNV-RP-C203* [4]) in seawater with cathodic protection. Figure 3 is provided for reference of joint location terminology used in Table 3.

Table 3 – Calculated fatigue life.

Group	Joint	Connection	Location	Membrane stress [MPa]	Bending stress [MPa]	Hot spot stress [MPa]	Fatigue Life [Yr]	Allowable Stress [MPa]
1	J1	BT-LS	Brace	151	84	235	5	229
2	J1	BT-LS	Chord at crown	130	58	188	12	
3	J1	BT-LS	Chord at saddle	188	62	250	4	235
4	J1	BT-KB	Brace	140	90	230	4	219
5	J1	BT-KB	Chord at crown	153	42	195	10	
6	J1	BT-KB	Chord at saddle	172	125	297	2	235
7	J2	P-KB	Brace	146	104	249	2	203
8	J2	P-KB	Chord at crown	69	163	232	7	
9	J2	P-KB	Chord at saddle	45	68	114	151	
10	J2	P-KB	Long'l bhd*	186	3	189	6 *	
11	J3	P-NT	Brace	78	79	157	14	
12	J3	P-NT	Chord at crown	47	11	58	1456	
13	J3	P-NT	Chord at saddle	122	162	284	2	203
14	J3	P-US	Brace	131	127	258	4	242
15	J3	P-US	Chord at crown	39	29	68	664	
16	J3	P-US	Chord at saddle	111	50	161	12	
17	J3	P-LS	Brace	98	133	231	3	203
18	J3	P-LS	Chord at crown	114	52	167	11	
19	J3	P-LS	Chord at saddle	101	60	161	13	
20	J3	NT-US	Brace	207	85	291	3	242
21	J3	NT-US	Chord at crown	122	14	136	26	
22	J3	NT-US	Chord at saddle	179	92	271	2	203
23	J3	NT-LS	Brace	189	106	295	1	203
24	J3	NT-LS	Chord at crown	86	15	101	100	
25	J3	NT-LS	Chord at saddle	167	13	181	8	
26	J3	NT-LS	Long'l bhd*	182	3	185	5 *	

Notes: Connection defined as Chord-Brace with the following abbrevations:
BT = Ballast Tank KB = Knee Brace NT = Nacelle Tube
LS = Lower Spar P = Pontoon US = Upper Spar
* Longitudinal bulkheads inserted locally in way of the joint. FEA membrane stress scaled down linearly with plate thickness. Bending stress scaled quadratically.
Group 10 insert 1/2" plate
Group 26 insert 3/4" plate

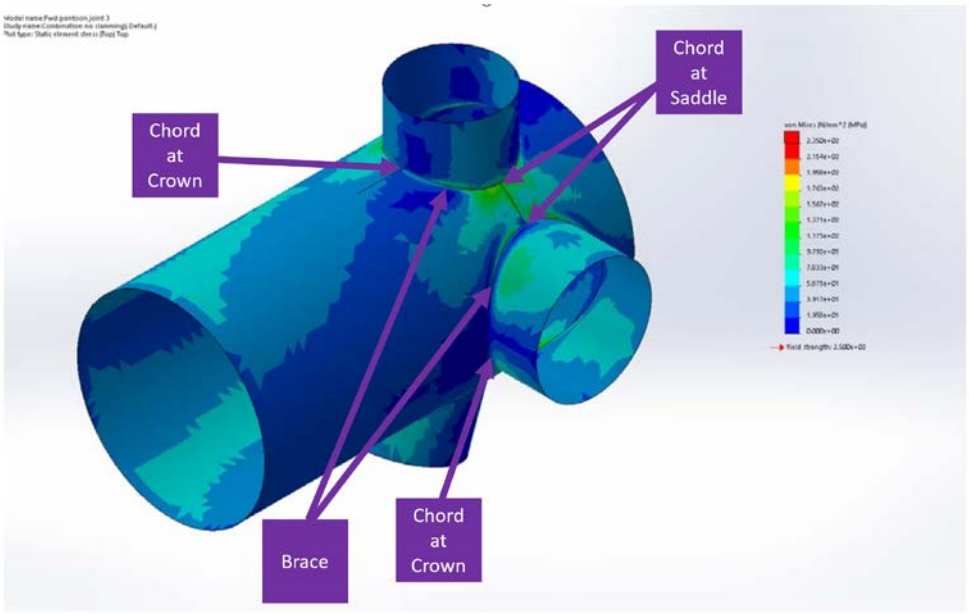

Figure 3 – Von Mises stress of aft, inboard side of forward pontoon joint.

The maximum stress range assumes that the hot spot stresses are fully reversing. The characteristic stresses reflect the 50-year return period of the extreme sea state in *M2.1-Design Load Cases for Structural Optimization* [2]. The average zero-upcrossing period was calculated for the WETS site from the wave scatter diagram in *M2.1-Design Load Cases* [2] and an assumed wave period ratio (Tz/Te) of 0.71. The calculations assume that the wave zero-upcrossing period is representative of the load and stress response period.

The design did not initially achieve a 5-year fatigue life based on this conservative, simplified fatigue life estimate. Longitudinal bulkheads in way of the joints were inserted locally (example in Figure 4 below) with thicker plate to achieve a 5-year fatigue life. Increasing plate thickness to reduce stress does not improve fatigue life in all cases, because allowable stress reduces as the thickness increases. Table 3 also provides the maximum allowable stress for a 5-year fatigue life for use in evaluating potential structural design modifications.

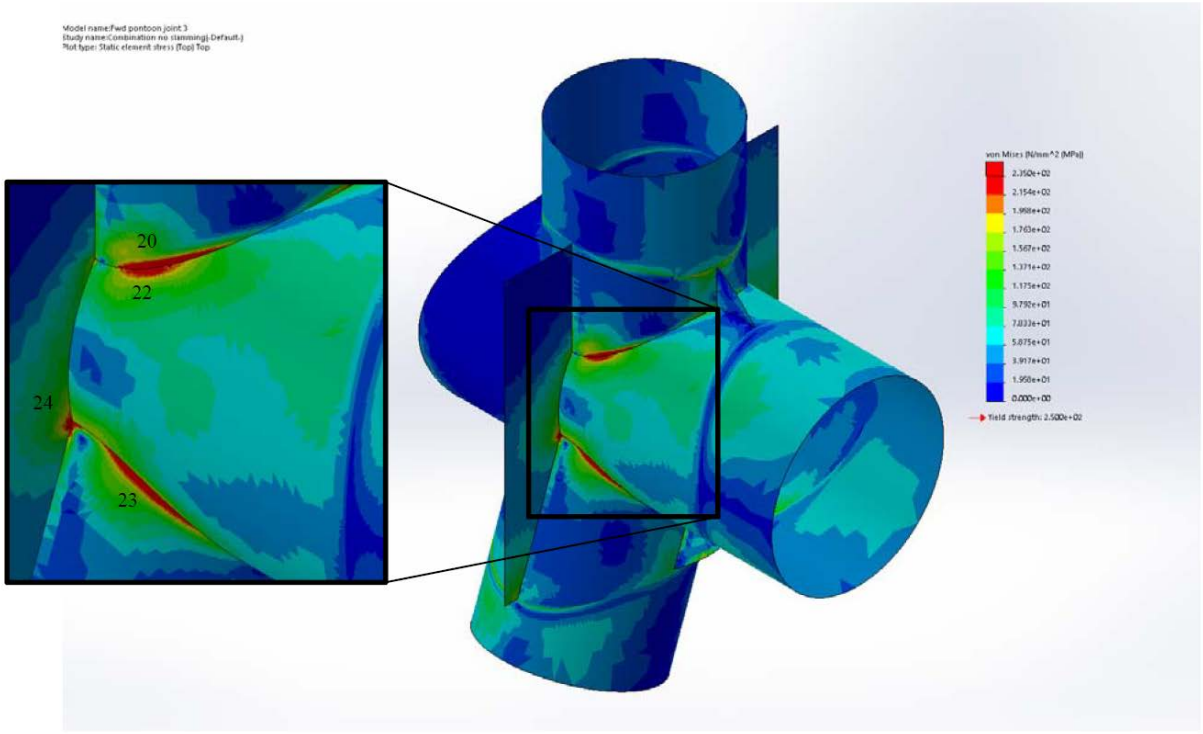

Figure 4 – Von Mises stress of forward pontoon joint, with closeup (shell removed for clarity).

Improved welds offer an approach to increase fatigue life. DNV allows the use of weld profiling but discourages weld toe grinding or hammer peening at the design stage. Table 4 shows that the minimum calculated fatigue life of the WEC increases to five years if weld profiling is applied. Full penetration welds at the joints are required for this approach.

Table 4 – Calculated fatigue life with weld profiling.

Group	Joint	Connection	Location	Membrane stress [MPa]	Bending stress [MPa]	Hot spot stress [MPa]	Profiled stress [MPa]	Fatigue Life [Yr]	
1	J1	BT-LS	Brace	151	84	235	173	15	**
2	J1	BT-LS	Chord at crown	130	58	188	138	43	
3	J1	BT-LS	Chord at saddle	188	62	250	182	13	**
4	J1	BT-KB	Brace	140	90	230	170	14	**
5	J1	BT-KB	Chord at crown	153	42	195	142	38	
6	J1	BT-KB	Chord at saddle	172	125	297	220	6	**
7	J2	P-KB	Brace	146	104	249	185	9	**
8	J2	P-KB	Chord at crown	69	163	232	177	17	
9	J2	P-KB	Chord at saddle	45	68	114	86	501	
10	J2	P-KB	Long'l bhd*	186	3	189	135	22	*
11	J3	P-NT	Brace	78	79	157	117	61	
12	J3	P-NT	Chord at crown	47	11	58	42	9205	
13	J3	P-NT	Chord at saddle	122	162	284	213	5	**
14	J3	P-US	Brace	131	127	258	193	11	**
15	J3	P-US	Chord at crown	39	29	68	51	3701	
16	J3	P-US	Chord at saddle	111	50	161	118	59	
17	J3	P-LS	Brace	98	133	231	174	11	**
18	J3	P-LS	Chord at crown	114	52	167	122	50	
19	J3	P-LS	Chord at saddle	101	60	161	119	58	
20	J3	NT-US	Brace	207	85	291	213	7	**
21	J3	NT-US	Chord at crown	122	14	136	97	145	
22	J3	NT-US	Chord at saddle	179	92	271	199	6	**
23	J3	NT-LS	Brace	189	106	295	218	5	**
24	J3	NT-LS	Chord at crown	86	15	101	73	614	
25	J3	NT-LS	Chord at saddle	167	13	181	129	39	
26	J3	NT-LS	Long'l bhd*	182	3	185	132	18	*

Notes: Connection defined as Chord-Brace with the following abbrevations:
BT = Ballast Tank KB = Knee Brace NT = Nacelle Tube
LS = Lower Spar P = Pontoon US = Upper Spar
* Longitudinal bulkheads inserted locally in way of the joint.
** **Weld profiling required to achieve 5-yr fatigue life.**

The images provided by Glosten from the Von Mises stress analysis allow C-Power to minimize the linear distance of weld profiling by restricting application to areas of significant stress. The longitudinal bulkheads added during the fatigue analysis provided the location of sustains to which rigging fixtures and equipment could be added to the structure design.

Lifting points were designed to facilitate assembly and shipping. The lifting arrangement consists of two lifting pad eyes on the aft bulkhead of each pontoon. The lifting pad eyes were designed to the estimated lightship weight of the WEC without the permanent ballast. A 1.5 dynamic load factor was assumed to allow lifts in sheltered waters. Each pad eye is rated for 372 kips (169 t). Crosby 200 t Wide Body Shackles with 1-1/8" 6x37 IWRC EIPS Wire Rope are assumed to attach to each lifting eye vertical to world. The resulting angle of 22° from the pontoon axis trims the WEC slightly bow down (~4°) with respect to the WEC's cribbing orientation. The same lifting eye and shackle may be used to lift each fully outfitted pontoon/spar/knee assembly. The notional lifting arrangement is depicted in the following figure.

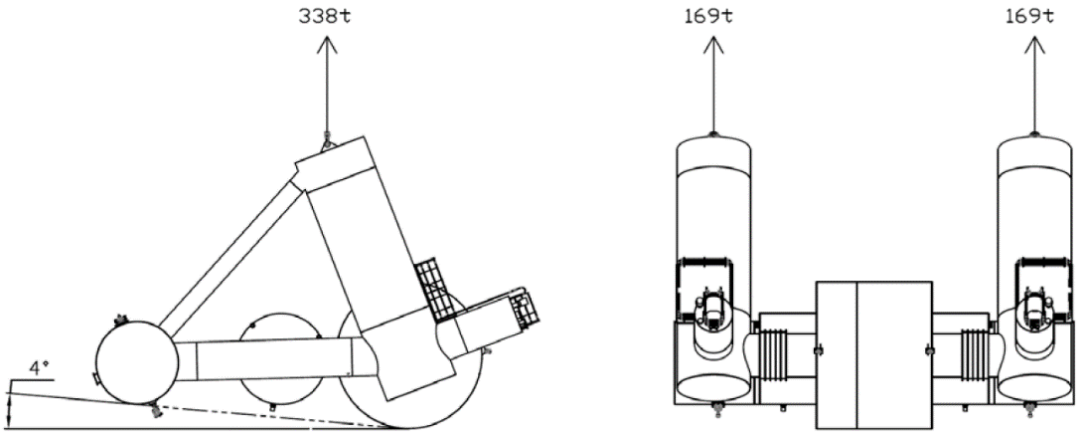

Figure 5 – Lifting and rigging.

First principles were used to size the pad eye and an FEA was performed to verify the support structure. The longitudinal bulkhead ¾" inserts in way of the lifting eye were assumed to be NV AH36 steel and all other structure NV A. Results indicated the longitudinal bulkhead in way of the knee brace pipe backing structure was needed to run continuously through the pipe

The WEC may be lifted or rolled onto a deck cargo barge. The WEC is assumed to be moved and stowed (for shipping or dry docking) in approximately the towed orientation in order to facilitate deployment. Note, this results in all equipment and platforms being off-axis by more than 60°. The lower point of ballast tank and nacelle cylinders is assumed to be 2m off the ground/deck.

WEC support and tiedown was designed such that the WEC could be transported on a cargo barge. The blocking and sea fastening arrangement was developed in accordance with *DNV-OS-H202 Sea Transport Operations* [5]. Three load cases are evaluated representing either the worst-case roll, pitch, or combination of the two from quartering seas. The resulting inertial loads are resisted by the blocking, seafastenings, and lashings. Overturning moments are countered by variable blocking pressures. Lateral loads are absorbed by friction. Lateral loads that exceed the friction forces are reacted by the seafastenings. The predicted accelerations do not tip the overall WEC, but there are localized uplift loads that are countered by the lashings.

Blocking and seafastenings are assumed to be capped with wood dunnage to evenly distribute loads into the WEC. The DNV standard limits the pressure applied to wood dunnage to 2 MPa. The highest blocking pressures occur when heave is positive which increases the effective vertical load. The maximum seafastening loads occur when heave is negative since that minimizes the effective vertical load and results in less of the lateral inertial load being absorbed by friction.

The mooring and towing fittings and respective support structures were designed in accordance with the *DNV-OS-E301 Position Mooring* [6]. Glosten designed the mooring fittings size to accommodate the minimum breaking strength of mooring line of 1480 kN (151 t) which CPower provided.

The WEC ballast tank (main drag-inducing component) has an approximate drag of 8 t at 3.5 knots. A load factor of 1.5 was assumed to account for wave-making drag, and wave and wind loading resulting in a 12 t tow load. The minimum breaking strength of the tow line is assumed to be 3 times the tow load, or 36 t. The towing fittings design is based on the breaking strength of the line.

RUD VRBS 50 t and VRBS 16 t load rings were selected as the mooring and towing fittings, respectively; the hinge design will better manage the varying load angles. The rings are welded to base plates that stand

off from the hull on foundation pedestals shown below in Figure 6. This was done to preclude interference between the shackle and hull. First principle stress and beam analyses were performed to size the pedestals and hull internal backing structure. All structure was assumed to be NV A steel. The umbilical connection design was extended from the aforementioned mooring attachments as the loads were assumed to be comparable.

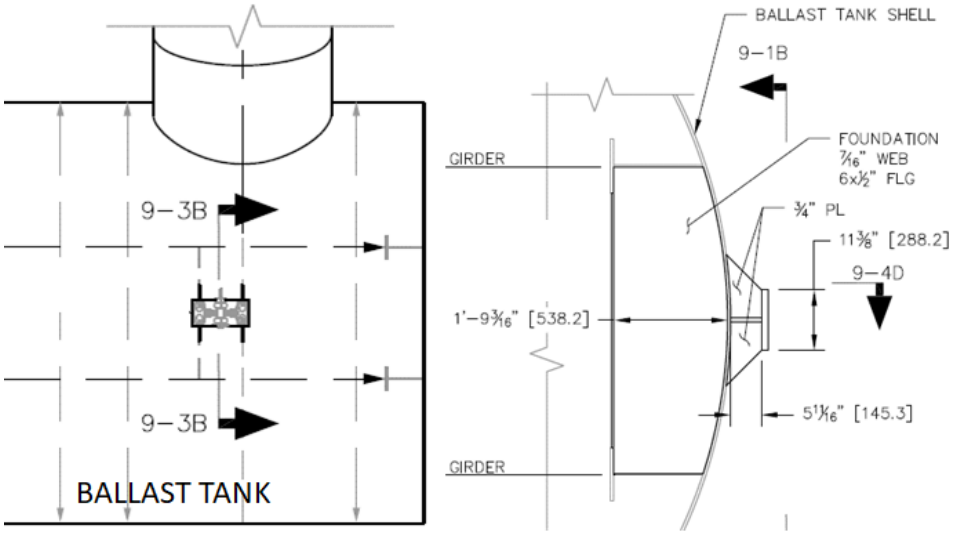

Figure 6 - Foundation pedestals.

The ballast system functions to control the attitude and stability of the WEC. The permanent ballast tank is subdivided (port to starboard); each subdivision is partially filled with sand, and the remainder flooded with fresh water. Permanent ballast is designed to be filled with the WEC floating horizontally; once filled the permanent ballast tank is sealed. The two variable ballast tanks are designed to be flooded with seawater; as they fill, the ballast tank rotates downward bringing the WEC to its vertical, power production orientation. The ability of the WEC to transition between floating tow and power production configurations via a seawater ballast change, without the need for any external floatation, is a significant step forward from the previous (Baseline) design. Variable ballasting also allows the structure to achieve optimal freeboard (amount of structure above the waterline) and roll (by filling port or starboard variable tank more with respect to the other) to accommodate center-of-gravity (CG) offsets and unintended mass differences between design and fabrication. This greatly improves the flexibility of fabrication and deployment while reducing overall structure tolerances and CG balancing

Intact stability was assessed in both the power production and towing orientations. The WEC is subdivided into 11 watertight compartments and damaged stability analysis validates the design requirement that any one compartment may flood without the WEC sinking or becoming unstable.

The structural analysis and design of the prototype H2 are covered in detail in *CPower WEC Design Documentation* [7] and *CPower WEC Structural Arrangement* [8].

3 GEOMETRIC AREAS OF INTEREST FOR FURTHER DEVELOPMENT

The WETS H2 prototype is a significant step forward for C·Power's StingRAY WEC technology. The advantages of the next-generation H2 hull represent significant progress on the Project objectives of increased Power to Weight Ratio and decreased Levelized Cost of Energy.

Engineers from C·Power, Glosten, and the National Wind Technology Center worked together to identify geometric areas of interest in the StingRAY H2 hull design that could be further developed and tested. The

overall project goal is to reduce WEC mass, with a secondary goal of reducing WEC construction and material cost. Three criteria were used in assessing potential GAIs (see Figure 1), ensuring that the proposed optimization would be informative, practical, and achievable:

- Potential Impact on Project Objectives
    - Clearly, it is important that any further efforts made within the Project have significant impact on the Project objectives.
- Test Facility Capabilities
    - The National Wind Test Center (NWTC), itself a part of the National Renewable Energy Laboratory (NREL), had been contracted to perform structural testing in support of the Project; thus, the capabilities of the NWTC test facility were considered alongside GAIs.
- Schedule and Budget
    - Practically speaking, the remaining Project schedule and budget were also considered in light of the GAIs and associated testing and analysis.

Figure 7 – Criteria for the selection of geometric areas of interest for further optimization.

Although a number of other ideas were discussed, there were two leading concepts for the physical test to satisfy both feasibility and project usefulness.

The arm of the drive float was particularly of interest for development and the interface with the nacelle-housed power take-off system. The geometry is complex in this region and the loading is severe and multi-dimensional as it traveled through its normal and maximum range of motions. The loading in this area led to a conservative design approach. The design relies on relatively thick plate and substantial internal and external stiffening elements to survive the dynamic loading. Testing of this area would provide useful data in further development into the geometry of the drive arm, scantlings, and attachment to both the float, bearings, and power generator.

A test program aiming to optimize this design would certainly be interesting but would be prohibitively costly and difficult to test at NREL. A single test specimen fabricated to represent the float/arm/ nacelle interface at full-scale would be large and costly. The structural analysis was based on design loads representing five unique stress states that would need to be tested. In any test program, multiple identical tests are required to confirm the soundness of the testing methodology. Each test to failure would yield a single data point. Also, development of the drive float arm did not best support the project goals to reduce mass and fabrication costs, as it was a relatively small area in comparison to the WEC as a whole.

It was decided by the collaborative team of engineers that the geometric area of interest that had the greatest potential of mass reduction to the WEC structure was to incorporate Fiber-Reinforced Plastic (FRP) shells into the StingRAY H2 hull design.

Composite materials provide tremendous benefits in the marine environment, including corrosion resistance, very low levels of required maintenance, high fatigue life, and high potential weight savings. However, because composite laminates require human input in the form of chemical mixing and consolidation, it is recommended to quantify the physical properties of the as-built laminate and derive as-built design values. Testing directly addresses these vagaries so that design can optimize the advantages of the technology and minimize the risks. The steel-to-composite joint is the least understood structural element and therefore represents the highest risk. Coupon and full-scale joint tests could mitigate these risks.

A decision was made to pursue a mixed materials approach to reducing structural mass and cost. Several subcomponents were identified in which there were structural spans whose simple shapes would be readily fabricated from mandrel-wound FRP. It was hypothesized that by substituting FRP for steel where appropriate, significant cost and weight savings would be realized. Investigation and testing of FRP shell on the pontoons offered significant mass reduction. The large-diameter cylinders that make up most of the pontoon structure are a common structure, routinely produced by automated filament winding for several other industries. The use of this proven manufacturing process could reduce fabrication cost significantly in comparison to steel fabrication techniques. Additionally, positive results in testing FRP pontoons and joints applications would directly transfer to similar components in the WEC design to include but not limited to the knee braces, spars, and ballast tank.

After further development on the concept, adapting the StingRAY H2 hull design to accommodate the filament wound FRP shells proved to be difficult and require testing of the joint construction. Connecting the FRP shells to the steel structure required two major factors to be addressed. The primary opportunity for research and testing was the design of a large, high-stress and fatigue-life, watertight, FRP to steel joint. Available information on FRP-to-steel joint design did not directly transfer to the application of large diameter subcomponents. The low-tolerances structures required, commonly produced by automated filament winding (± 1 inch in diameter and up to 34% material thickness per Ershigs) were incompatible with the tighter tolerances used in steel structure fabrication. Costs estimated to implement and install the FRP shell subcomponents stood to increase fabrication cost over the current steel pontoon design, despite the much lower manufacturing costs. In order to successfully complete the project goals of mass reduction and cost reduction, an extremely low-tolerance, high-stress and fatigue-life, watertight FRP-to-steel joint had to be designed and validated.

The required number of articles to confirm test soundness is typically prohibitively expensive for mesoscale (testing that utilizes a complete, scaled version of the object under design, often utilizing multiple concurrent loads testing). Instead, design engineers utilized standardized testing methods to obtain design values. Using these standardized methods provides a cost-effective way to characterize the materials and inform design decisions. Design values can be derived from coupon tests to obtain the strength and stiffness for a given laminate as well as accounting for the variability of composite layup for each fabricator. The variables of interest include tension, compression, lap shear, flexure, and possibly fatigue and shock loading. A matrix of coupon tests efficiently characterized the design space and allow the design engineers to optimize the design for a component with reduced mass and cost while increasing reliability.

To best utilize the remaining *schedule and budget*, a robust test plan consisting of coupon and full-scale sectioned joint testing was conceived. The draft test plan was developed in consultation with NREL, ensuring that the work was within the *test facility's capabilities*. The mixed material concept design is discussed in greater detail in the following sections.

4 MIXED MATERIAL PONTOON CONCEPT DESIGN

The design laminate is a simple cylinder with a monolithic layup schedule based on processes from Ershigs, a long-time FRP fabrication partner of C·Power. The Ershigs process for large filament-wound (FW) tanks is to use a spray chop gun to add chopped strand mat (CSM) as the first layer against the mandrel, and then consolidate over that CSM with a full layer of filament-wound e-glass. Consecutive double layers of filament windings are added interspersed with a hand laid stitched fiberglass unidirectional fabric (U, or UNI) supplied by Vectorply. FW angles are specified at $\pm 65°$ from the mandrel axis, and a single layer comprises windings in both directions. The unidirectional fabric is oriented with the fibers parallel to the mandrel axis. Note that the CSM does not contribute structurally to the laminate, and the fabricator may use it to maintain laminate quality as necessary. An epoxy vinyl-ester resin is specified.

The concept laminate was developed by Glosten, guided by *DNVGL-ST-C501 Composite Components* [9]. The Tsai-Wu failure criterion (TWFC) was used to evaluate laminate failure in lieu of maximum strain requirements; the equations used to evaluate 2D TWFC are given in Figure 8.

$$R^2\left(F_{11}\sigma_1^2 + F_{22}\sigma_2^2 + F_{12}\sigma_{12}^2 + 2H_{12}\sigma_1\sigma_2\right) + R\left(F_1\sigma_1 + F_2\sigma_2\right) < 1$$

$$R = \gamma_F \cdot \gamma_{Sd} \cdot \gamma_m \cdot \gamma_{Rd}$$

$$F_{11} = \frac{1}{\hat{\sigma}_{1t}\,\hat{\sigma}_{1c}}, \quad F_{22} = \frac{1}{\hat{\sigma}_{2t}\,\hat{\sigma}_{2c}}, \quad F_{12} = \frac{1}{\hat{\sigma}_{12}^2}$$

$$H_{12}^* = \frac{H_{12}}{\sqrt{F_{11}F_{22}}}, \quad F_1 = \frac{1}{\hat{\sigma}_{1t}} - \frac{1}{\hat{\sigma}_{1c}}, \quad F_2 = \frac{1}{\hat{\sigma}_{2t}} - \frac{1}{\hat{\sigma}_{2c}}$$

where:

n	ply co-ordinate system direction
σ_n	characteristic value of the local load effect of the structure (stress) in the direction n
$\hat{\sigma}_{nt}$	characteristic tensile strength in the direction n
$\hat{\sigma}_{nc}$	characteristic compressive strength in the direction n
$\hat{\sigma}_{nk}$	characteristic shear strength in the direction nk
γ_F	partial load effect factor
$\gamma_{Sd,}$	partial load-model factor
γ_M	partial resistance factor
γ_{Rd}	partial resistance-model factor

Figure 8 – Tsai Wu Failure Criterion (DNVGL-ST-C501).

The safety factor, R, is calculated as the product of several partial safety factors. A combined partial load and resistance safety factor of 1.11 was specified (for known maximum load effects), a partial load-model factor of 1.0 was specified (as FEA was used), and a partial resistance model factor of 1.15 was specified (for degraded properties). A sensitivity study of the model with the factor H_{12} = 0, -0.5, and 1 was completed with little difference in the results, so -0.5 was used. To simplify FEA processing, the inequality above is simplified so that R is squared in both terms. This is conservative because R > 1.0. Dividing by the R^2 term on both sides gives the TWFC limit must be less than 0.61.

Siemens Femap 11.4.2 with NX Nastran is used to mesh, analyze, and post-process the geometry. The FEA model geometry is taken as the 7.7m pontoon length between the adjacent steel joints (see *CPower WEC Structural Arrangement* [8]). The pontoon is modeled as a 3.8m diameter cylinder. The global coordinate system is X along the cylinder axis, Y in the waterplane, and Z vertically up. The element coordinate system is cylindrical with z acting along the cylinder axis, t tangent to the cylinder, and r radial. Each element is aligned with the cylinder axis. Elements are laminate plate elements nominally 25mm square.

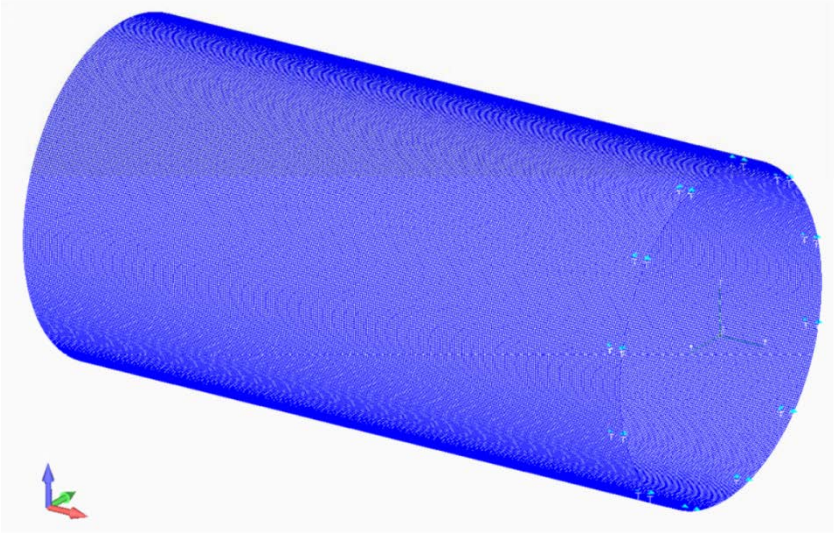

Figure 9 – Pontoon finite element model (FEM).

The materials modeled are developed from manufacturers' specification sheets, with some corrections applied following *DNVGL-ST-C501* [9]. The boundary conditions model the steel structure with its flange connection. The load cases are derived from the *WEC Design Documentation* [7] and are listed below in Table 5.

Table 5 – Concept pontoon design load cases.

LC	Description	FX (kN)	FY (kN)	FZ (kN)	MX (kN-m)	MY (kN-m)	MZ (kN-m)	BC	Pressure
1	Max Bending Transverse Shear	-161	876	0	35	7755	-6643	A	Hydro
2	Max Shear Transverse	-497	894	0	48	4761	-6780	A	Hydro
3	Max Axial Tension Transverse Shear	468	619	0	-152	3601	-4694	A	Hydro
4	Max Axial Compression Transverse Shear	-866	426	0	64	518	-3231	A	Hydro
5	Max Torque Transverse Shear	-155	372	0	299	705	-2821	A	Hydro
6	Slamming	0	0	0	0	0	0	B	Slam
7	Max Bending Vertical Shear	-161	0	876	35	1112	0	A	Hydro
8	Max Shear Vertical	-497	0	894	48	-2019	0	A	Hydro
9	Max Axial Tension Vertical Shear	468	0	619	-152	-1093	0	A	Hydro
10	Max Axial Compression Vertical Shear	-866	0	426	64	-2713	0	A	Hydro
11	Max Torque Vertical Shear	-155	0	372	299	-2116	0	A	Hydro

For all load cases, the pontoon cylinder is fixed at the near end in translation and rotation. This approximates the 150mm steel flange connection and results in the maximum loads occurring at the joint between the composite and steel structures. For the slamming load case only (LC 6), the far end is supported in translation and rotation around the transverse and vertical axes (Y and Z). This better approximates the support of the steel structure at the far end of the pontoon during a slamming load.

Loads are applied through a rigid body element at the far end of the cylinder. This rigidness approximates the steel assembly the pontoon is connected to and ensures that the maximum fiber strains are acting on the near-end joint. Load Cases 1-5 assume the maximum shear load acts in the waterplane and includes a corrective moment about the vertical axis. Load Cases 7-11 assume the maximum shear direction acts vertically and include a correction to the transverse axis moment. Figure 10 shows the hydrostatic loads and boundary conditions.

All load cases include hydrostatic water pressure acting perpendicular to the surface from the midplane down proportional to the depth of water (vertical axis) except Load Case 6. Load Case 6, Slamming includes a 134 kPa pressure on the bottom 60˚ chord of the cylinder only as shown in Figure 11.

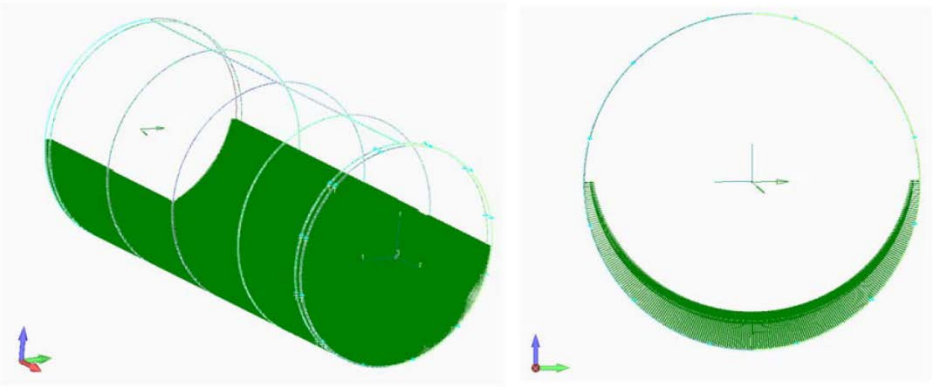

Figure 10 – Hydrostatic pressure load case applied forces vary with depth.

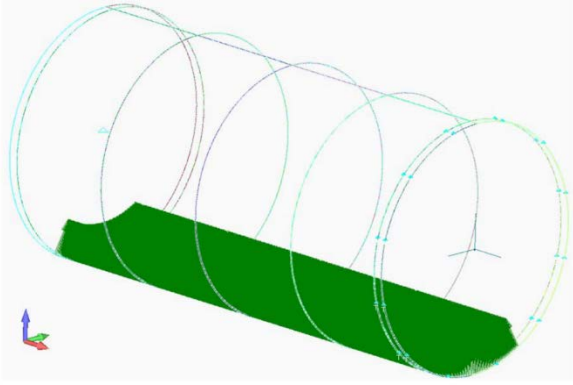

Figure 11 – Slamming load case applied forces are constant.

The reaction loads at each boundary condition node are taken and applied to a discretized bondline 75mm long, and 25mm wide, corresponding to the nodal spacing and half the assumed flange width. The axial and tangential loads dominate and act as shear stresses in the bondline, while the radial force results in

tension stress. To quantify the required strength of the adhesives, the shear and radial stresses are combined to find a required tensile (cohesive) strength.

A summary of maximum TWFC for each load case is presented in Table 6, and Table 6 – Maximum TWFC summary.

LC	Description	TWFC
1	Max Bending Transverse Shear	0.29
2	Max Shear Transverse	0.26
3	Max Axial Tension Transverse Shear	0.13
4	Max Axial Compression Transverse Shear	0.06
5	Max Torque Transverse Shear	0.04
6	Slamming	0.52
7	Max Bending Vertical Shear	0.08
8	Max Shear Vertical	0.04
9	Max Axial Tension Vertical Shear	0.02
10	Max Axial Compression Vertical Shear	0.01
11	Max Torque Vertical Shear	0.005

Table 7 details the maximum resultant discretized bondline stresses. The FEA results were used to specify a concept layup schedule and required adhesive strength. The limiting load case for both the laminate and the adhesive joint is the slamming load case. The concept layup schedule is 26mm thick solid laminate [3.0oz CSM, 1FW, 9(1U,2FW), 1.5oz CSM].

The bondline loading is dominated by shear (see Figure 12). Based on these results, and adding a safety factor equivalent to the TWFC, the adhesive strength shall be at least 30.5 MPa (= 18.6 MPa / 0.61) in a wet-fatigued condition. An adhesive that fit the requirements was not found, so it is recommended to use a double lap shear joint which will reduce the required adhesive strength by half to 15.3 MPa. The double lap shear detail is preferred over an extension of the steel flange because it adds additional robustness. It is found that as the flange gets longer, the inboard edge attracts more load which strains the bondline load distribution assumptions. Additionally, since the double lap joint will utilize adhesive on both sides of the pontoon laminate, the adhesive bondline thickness will be better controlled for geometric deviations between the steel flanges and the pontoon circumference. It is expected that bondline thickness will play an important role in the characteristic strength of the adhesive, so this is important to quantify in future testing programs.

Table 6 – Maximum TWFC summary.

LC	Description	TWFC
1	Max Bending Transverse Shear	0.29
2	Max Shear Transverse	0.26
3	Max Axial Tension Transverse Shear	0.13
4	Max Axial Compression Transverse Shear	0.06
5	Max Torque Transverse Shear	0.04
6	Slamming	0.52
7	Max Bending Vertical Shear	0.08
8	Max Shear Vertical	0.04
9	Max Axial Tension Vertical Shear	0.02
10	Max Axial Compression Vertical Shear	0.01
11	Max Torque Vertical Shear	0.005

Table 7 – Bondline stresses.

LC	Description	Bondline Stress (MPa)
1	Max Bending Transverse Shear	17.9
2	Max Shear Transverse	17.1
3	Max Axial Tension Transverse Shear	12.1
4	Max Axial Compression Transverse Shear	8.4
5	Max Torque Transverse Shear	6.7
6	Slamming	18.6
7	Max Bending Vertical Shear	9.2
8	Max Shear Vertical	6.1
9	Max Axial Tension Vertical Shear	4.7
10	Max Axial Compression Vertical Shear	1.6
11	Max Torque Vertical Shear	1.0

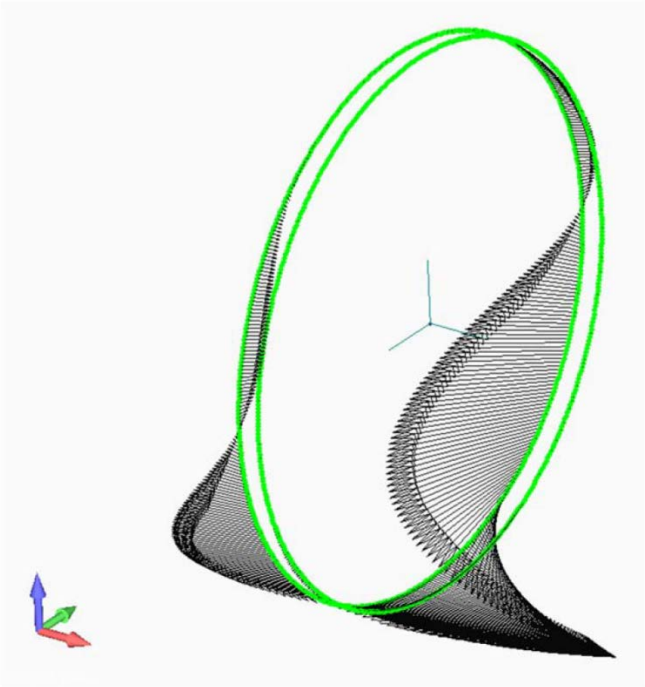

Figure 12 – Resultant bondline force vectors at the near-end boundary conditions, load case 6.

The concept joint design is an adhesively bonded double lap consisting of two steel rings capturing the edge of the composite shell (Figure 13). The connection joints between the composite cylinder and the adjacent steel structure are designed to be fault-tolerant and simple to assemble. A 45° angle is specified at the terminus of the adhesive to minimize cleave and peel forces.

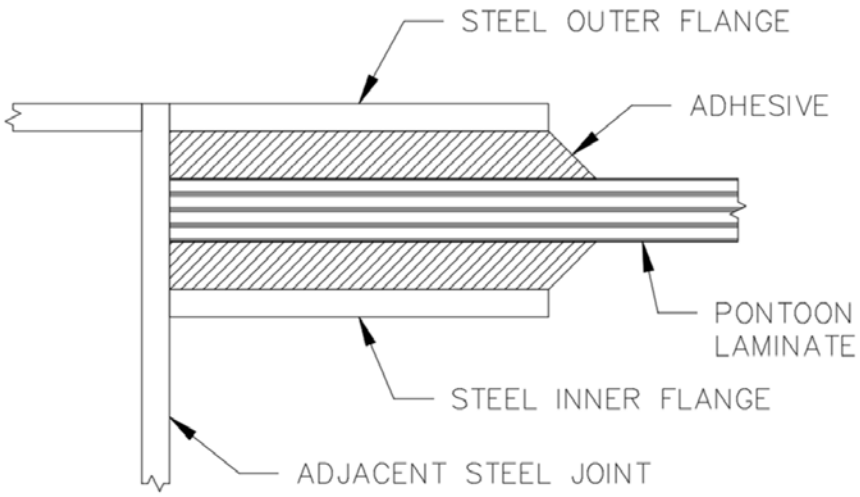

Figure 13 – Double lap shear joint detail.

The concept design of the hybrid structural subcomponent (i.e., the test article) is described in detail in *Test Article Design Technical Memo* [10].

5 CONCLUSION

The next-generation hull architecture significantly increases the power performance of the WEC, while reducing the complexity and cost of the WEC system through efficient use of structural and power generation components, along with simplified component geometries aimed at reducing manufacturing costs. Under 6610, the prototype H2 WEC design was progressed from concept to final design with structural drawings, in preparation for a planned deployment offshore of the MCBH at WETS. The new design eschews the costly steel ballast utilized by the Project Baseline WEC, in favor of low-cost concrete and seawater ballast.

Assessment of the H2 design resulted in several Geometric Areas of Consideration for further optimization. Three criteria were used to down-select for testing and optimization: potential impact on Project objectives; test facility capabilities; and available schedule and budget.

A decision was made to pursue a mixed materials approach to reducing structural mass and cost. This approach substitutes FRP for steel where appropriate, resulting in cost and weight savings. An adhesive, double lap shear joint is used to join the FRP and steel subcomponents. The benefits of steel are maintained where most useful, for instance at structural joints where the stiffness of steel is required, and the complex geometry is more readily fabricated with steel. However, there are structural spans whose simple shapes are readily fabricated with mandrel-wound FRP and where significant cost and weight savings can be found.

The concept design comprises a cylinder with a monolithic FRP layup schedule, adhesively bonded to a double lap consisting of two steel rings capturing the edge of the composite shell.

6 REFERENCES

[1] “Design requirements for marine energy systems,” International Electrotechnical Commission, IEC 62600-2, Ed. 1, Aug. 2016.

[2] “Design Load Cases for Structural Optimization,” Columbia Power Technologies, DE-EE0006610-MS2.1 v2.0, Jul. 2016.

[3] “StingRAY Design Loads,” Columbia Power Technologies, DE-EE0006610 SR-DesignLoads v2.1, Mar. 2018.

[4] “Fatigue Design of Offshore Steel Structures,” DNV, DNV-RP-C203, 2014.

[5] “CPower WEC Design Documentation,” Glosten, 18024-10-100 Rev. A, Jun. 2018.

[6] “CPower WEC Structural Arrangement,” Glosten, 18024-100–01 Rev. B, Apr. 2019.

[7] “Composite Components,” DNV GL, DNVGL-ST-C501, Aug. 2017.

[8] “Test Article Design Technical Memo,” Glosten, 18024.01-200–01 Rev. A, Oct. 2018.